Food Research International 49 (2012) 702–709

Contents lists available at SciVerse ScienceDirect

Food Research International

journal homepage: www.elsevier.com/locate/foodres

Aroma delivery from spray dried coffee containing pressurised internalised gas

Tingting Yu [a], Bill Macnaughtan [a], Maxime Boyer [b], Robert Linforth [a], Keith Dinsdale [c], Ian D. Fisk [a,*]

[a] Division of Food Sciences, University of Nottingham, Sutton Bonington Campus, Sutton Bonington, Loughborough, Leicestershire, LE12 5RD, United Kingdom
[b] Agrosup Dijon, 26 Boulevard Petitjean, BP 87999, Dijon, FR 21079, France
[c] Mechanical Materials and Manufacturing Engineering, University of Nottingham, University Park, Nottingham, Nottinghamshire NG7 2RD, United Kingdom

ARTICLE INFO

Article history:
Received 8 June 2012
Accepted 22 August 2012

Keywords:
Coffee
Aroma
Gas entrapment
Hydration

ABSTRACT

A non-chemical, ingredient free method of enhancing aroma delivery during the preparation of instant coffee is presented. The approach detailed introduces a method for entrapping high pressure internalised gas within the pores of spray dried soluble coffee by cycling of both pressure and temperature. The headspace delivery of volatile aroma compounds during powder hydration was tracked by an atmospheric pressure chemical ionisation-quadrupole mass spectrometer, with a modified ion source. The release of pressurised gas on hydration caused a burst of volatile aroma compounds into the headspace, which was both faster (77%) and more intense (60%) than could be achieved using standard instant coffee or through the use of chemical effervescent agents alone (sodium hydrogen carbonate and citric acid). In addition, the process of natural gasification selectively accelerated the delivery of individual aroma compounds, with the time to maximum headspace intensity being reduced for both 2,3 butanedione and acetaldehyde.

1. Introduction

The drinking experience of soluble coffee is controlled by a number of sensory modalities including mouthfeel (Narain, Paterson, & Reid, 2004), hydration (Maughan & Griffin, 2003), thermal stimulus (Brown & Diller, 2008), physiological response (Quinlan et al., 2000), aroma (Bhumiratana, Adhikari, & Chambers, 2011) and taste (Geel, Kinnear, & de Kock, 2005). If one specifically considers aroma, there are several stages during preparation in which the aroma of the coffee can interact with the consumer: the opening of the jar (Jolly, Nacci, DeCeglie, & Vitti, 1972), mixing during preparation of the dried powder in the cup with water, orthonasal perception of the brew after preparation (Marin, Baek, & Taylor, 1999) and retronasal perception of the beverage on consumption (Denker et al., 2006). All the different stages play varying roles in perception, and crucially, all play a different role in distinguishing products, brands and roast and ground coffee from instant coffee. The delivery of aroma from the cup to the headspace at the stage of brewing will be the focus of this study as the author believes this is an often overlooked critical point of consumer differentiation between roast and ground coffee and instant coffee (Fisk, Kettle, Hofmeister, Virdie, & Silanes Kenny, 2012).

The technology that will be trialled in this study is that of natural gasification (Imison, 2011; Zeller, Ceriali, Gundle, 2006). Natural gasification of spray dried coffee can be achieved through exposing a spray dried powder to an elevated pressure and heating the coffee past its glass transition temperature (T_g). Once above T_g the coffee matrix becomes plasticised and increasingly permeable to the pressuring gas (Yampolskii, Pinnau, & Freeman, 2006), the pressurised gas is thereby internalised within the internal pore structure of the spray dried coffee. Cooling, whilst maintaining the gas pressure, allows the internalised gas to be entrapped due to the reduced gas diffusion coefficient (Schoonman, Ubbink, Bisperink, Le Meste, & Karel, 2002). Subsequent hydration of the spray dried coffee powder will depress the T_g (Franks, 1988; Saragoni, Aguilera, & Bouchon, 2007), leading to a rapid increase in gas mobility through the matrix (Kilburn et al., 2004) as the material moves from a rigid glassy state to a softened rubbery state, and release of the internalised gas into the hydrating medium. The process is schematically illustrated in Fig. 1 and the pore structure of a typical gasified coffee is demonstrated in Fig. 2.

In a practical example, the hydrating medium would be the water used to prepare a cup of instant coffee (Imison, 2011; Zeller et al., 2006), and the pressurised gas would be released during brewing. The gas would then rise to the surface and be either released or form a surface crema (foam) (Birsperink, Ufheil, Vuataz, & Schoonman, 2004; Imison, 2011; Kuypers, 1986; Panesar, Jeffs, & Turek, 1999).

The production of gas from a coffee powder and subsequent gas release from the liquid beverage will impact the beverage two fold. Firstly the production of gas will induce a movement in the dissolving powder which will increase mass transfer (Cussler, 1997) and increase the rate of dissolution of both bulk components (e.g. carbohydrates) and volatile aroma compounds; secondly, the release of gas to the headspace will increase the rate of transfer of aroma molecules from the liquid phase to the gas phase (Pollien, Jordan, Lindinger, &

* Corresponding author. Tel.: +44 115 951 6037; fax: +44 115 951 6142.
E-mail address: Ian.Fisk@nottingham.ac.uk (I.D. Fisk).

0963-9969
http://dx.doi.org/10.1016/j.foodres.2012.08.021

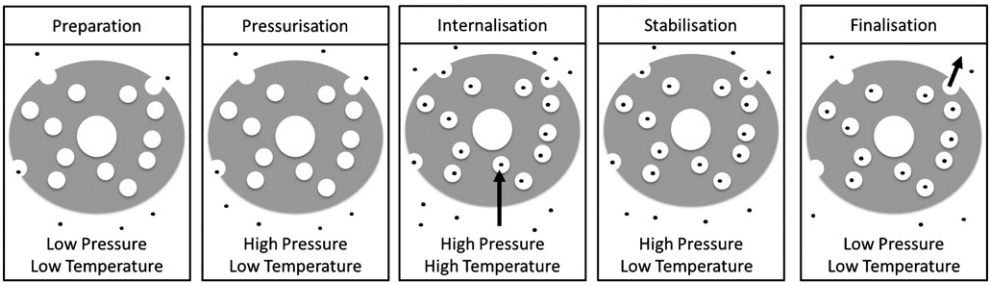

Fig. 1. Schematic illustration of spray dried coffee gas internalisation production process. Spray dried coffee is illustrated with internal and external pores in light grey and the pressurisation gas is illustrated as the black dots. The arrows illustrate the general trend for molecular movement of the gas molecules during the natural gasification process, which is separated into five phases (preparation, pressurisation, internalisation, stabilisation and finalisation).

Yeretzian, 2003). This is normally assumed to be due to an increase in the surface area (Taylor, 1998), the limiting factor in many food systems (Harrison, Hills, Bakker, & Clothier, 1997). This increase in surface area will drive any imbalances in the chemical potential between the gas and the liquid phase toward equilibrium and stabilise the concentration of headspace aroma.

Most supporting aroma chemistry literature in this research area originates from other fields. For example, carbonation increases the delivery of aroma in-vivo after the consumption of beer (Clark, Linforth, Bealin-Kelly, & Hort, 2011), gas bubble formation and release enhance the delivery of volatile compounds in champagne (Cilindre, Conreux, & Liger-Belair, 2011; Liger-Belair, Polidori, & Jeandet, 2008) and effervescent powders are proposed to enhance the delivery of volatile aromas in home fragrance devices (Lefenfeld, Berman, Berman, & Katz, 2003). There are no other aroma chemistry published works specifically in this area, although a study by Dold (Dold et al., 2011) investigated the impact of gas bubble formation in espresso coffee (Nespresso) on the delivery of flavour and identifies an enhanced flavour delivery as driven by gas bubble formation.

The aim of the overarching research program is to develop technologies that deliver flavour more effectively to the consumer. This is to be achieved through optimising delivery rate (Baek, Linforth, Blake, & Taylor, 1999; Linforth, Pearson, & Taylor, 2007), the temporal delivery profile (Fisk, Kettle, Hofmeister, Virdie, & Silanes Kenny, 2012; Xian & Fisk, 2012) and the total delivery yield (% of total flavour delivered in a perceivable gas form, rather than consumed aroma). The sub-program detailed herein evaluates the use of natural gasification of spray dried coffee to enhance aroma delivery and to modify the temporal delivery profile. A direct comparison is undertaken with a chemical effervescent agent to illustrate the potential of natural gasification.

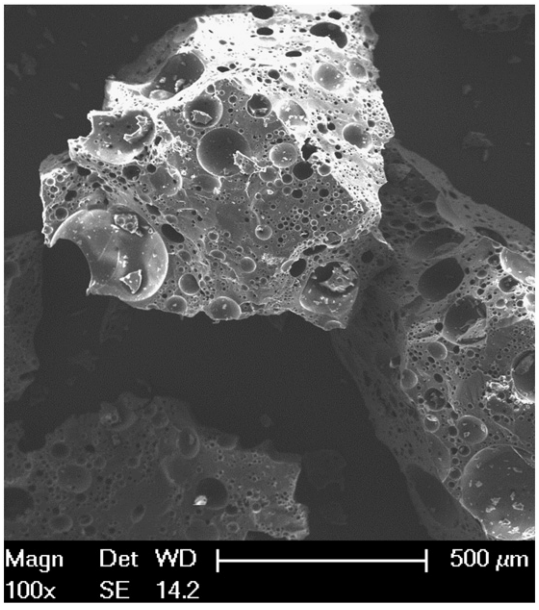

Fig. 2. High resolution scanning electron microscope image of spray dried coffee containing internalised gas. Coffee is fractured prior to analysis to illustrate internalised pore structure, which can be visualised as cavities of varying size on the exposed internal surface. White scale bar indicates 500 µm.

2. Materials and methods

Food grade sodium hydrogen carbonate, citric acid and instant spray dried coffee were purchased commercially. The pressure vessel used for gasification was purchased from Thar Technologies Inc., Pittsburgh, USA and the pressuring gas was analytical grade nitrogen (BOC, Nottingham, UK).

2.1. Natural gasification

Spray dried coffee (3 g) was added to a 10 mL stainless steel pressure vessel; the pressure vessel was pressurised with nitrogen to 40 bar and sealed. The pressure vessel was heated to a defined temperature (60 °C, 90 °C, 100 °C, 110 °C or 120 °C) and held for 10 min. The pressure vessel was then cooled to 30 °C in ambient air, depressurised slowly and the coffee containing internalised gas was isolated (Imison, 2011).

2.2. Scanning electron microscopy

Images were produced by a FEG SEM XL30 Philips SEM (USA). Samples were either analysed intact as a dry powder adhered to an adhesive base or crushed to allow viewing of the internal pore structure. Imaging was achieved by tungsten filament, secondary electron mode, spot voltage of 20.0 kV and spot size of 6.0.

2.3. Quantitative in-cup foam test

Foam volume was calculated by hydration of 1.5 g sample with 60 mL of tap water (Loughborough, UK) at 20 °C in a 100 mL glass cylinder (250 mm elevation and 25 mm diameter), water was added steadily over 5 s via funnel to facilitate controlled mixing (Imison, 2011). Foam volume (cm^3) was measured at time 1 min and time 10 min. Foam stability was calculated as the percentage retention when comparing foam volume at 1 min and foam volume at 10 min.

2.4. DSC

Thermal transitions were monitored using a heat flux Mettler Toledo Differential Scanning Calorimeter, model no. DSC 823e (Leicester,

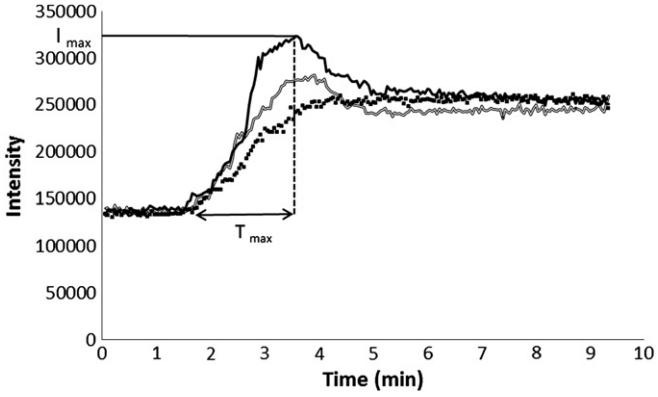

Fig. 3. Aroma release curve of spray dried instant coffee (1.5 g) hydrated in water (40 °C) (discontinuous dark line), coffee (1.5 g) with chemical effervescent agent (grey line) and coffee (1.5 g) with internalised gas (continuous dark line) by APcI-MS, I_{max} and T_{max} are indicated.

UK), with auto sampler and liquid nitrogen cooling attachment. Samples were sealed in stainless steel pans to ensure minimal changes in moisture content and run from −20 to 170 °C at scan rates of 10 °C min^{-1} with reheats being carried out. The machine was calibrated for temperature using the onset temperatures of melting of indium and cyclohexane, and for heat flow using the enthalpy of transition of indium. Glass transition temperature (T_g) values were calculated using Mettler Toledo Star^e software.

2.5. Aroma delivery

Aroma delivery was evaluated through the use of a bespoke powder dissolution cell connected to a standard APcI-MS headspace sampling interface (Fisk, Linforth, Taylor, & Gray, 2011b; Jublot, Linforth, & Taylor, 2005; Taylor, Linforth, Harvey, & Blake, 2000) via a heated transfer line (60 °C) to prevent condensation. The dissolution cell consisted of a 450 mL vessel with sample introduction and analysis ports fitted within the lid. The vessel had a 70 mm elevation, and contained the dissolution water and a magnetic stirrer (200 rpm). Samples (1.5 g coffee equivalent) were introduced through a cylindrical entry port and physically pushed under the surface of the water (40 °C) with a syringe plunger, to minimise contact with the headspace gas.

Samples chosen were standard instant coffee (1.5 g), coffee (1.5 g) treated at 60 °C, 90 °C, 100 °C, 110 °C or 120 °C and standard instant coffee (1.5 g) containing additional chemical effervescent agent (0.3 g, 0.6 g, 0.9 g, 1.2 g or 1.5 g at 2:1, sodium hydrogen carbonate:citric acid).

2.6. Headspace aroma analysis

The sample headspace was analysed by APcI-MS (Micromass, Manchester, UK) for 10 min at 30 mL/min with an MS nose interface (Micromass, Manchester, UK) and operated in full scan mode (m/z range 40–220) with a 4 kV corona discharge. The maximum intensity (I_{max}) and time to maximum intensity (T_{max}) were measured (Fisk et al., 2011b) as shown in Fig. 3 using a similar approach to that used previously (Fisk, Boyer, & Linforth, 2012).

A calibration curve was created with coffee preparations at a range of concentrations from 0.25 g to 30.0 g per 450 mL. Samples were allowed to equilibrate at 40 °C and the calibration curve was used to check for linearity within the range of analysis and to minimise any day to day variation. R^2 was acceptable at 0.95.

The mass spectral profile for all the samples contains significant numbers of a wide range of mass to charge ratios, of which 45, 68, 80 and 87 are tentatively identified, as previously described by Lindinger (Lindinger et al., 2005, 2008), as indicators of acetaldehyde, pyrrole, pyridine and 2,3 butanedione respectively. When comparing across the three samples, the mass spectrum at equilibrium was comparable for all m/z values apart from 61, which is tentatively identified as acetic acid and was elevated in the samples containing chemical effervescent agent. Total ion counts were recorded for all analyses to average out compound specific events.

2.7. Bulk density

Density was calculated by filling 10 cm^3, 15 cm^3 and 20 cm^3 volumetric cylinders with spray dried coffee and weighing the bulk weight of the coffee, then dividing the weight by the volume and averaging across the three volumes. All analyses were conducted in triplicate (Franca, Mendonça, & Oliveira, 2005).

2.8. Gas pycnometry

A helium pycnometer (Micromeritics AccuPyc-1330, Dunstable, UK) was used to determine the density of samples as purchased (powder density) and after physical disruption by manual grinding in a pestle and mortar for 60 s (crushed density). Density as purchased indicates the density of the sample including closed internal voids, and crushed density indicates the density of the continuous phase with internal voids removed.

2.9. Moisture content

The moisture content was determined by weighing the sample (~3 g) in pre-weighted aluminium trays, in triplicate, before and after 24 h in a convection oven MOV-112 F (Sanyo, Japan) at 105 °C.

2.10. Water activity

Samples were equilibrated to room temperature and the water activity was determined using the AquaLab series 3TE Water Activity Meter (Decagon Devices, Inc., USA) using the chilled mirror due point approach.

2.11. Hydrophobicity estimation by molecular modelling

Hydrophobicity was derived from estimated physicochemical properties of the volatile compounds of interest calculated using KOWWIN v1.67 within EPISuite ver. 3.20 (U.S. Environmental Protection Agency). Hydrophobicity was calculated as Log P, where Log P is taken as the logarithm of the predicted ratio of equilibrium concentration in two immiscible phases (octanol and water).

Log P was calculated for compounds of interest, for reference they are detailed in parenthesis as follows acetaldehyde (−0.17), 2,3 butanedione (−1.3), pyridine (0.8) and pyrrole (0.88).

2.12. Statistical analysis

All samples were analysed in triplicate in a randomised sample order and data was analysed by XLSTAT 2009 (Addinsoft, USA), using analysis of variance with Tukey's post hoc test to identify significant differences ($P<0.05$) within the samples (Fisk, White, Lad, & Gray, 2008).

3. Results and discussion

3.1. Structural analysis

The instant coffee under study is a spray dried carbohydrate enriched powder (moisture content was 4.98% ± 0.28% and water activity was 0.25 ± 0.002 at 24.5 °C) that contains a plurality of small

internal voids in the form of gas pores. Spray dried coffee is typically foamed by gas injection prior to drying to control product density, and additionally will form internal voids as a consequence of the movement of water during the rapid drying process. Scanning electron microscope (SEM) images were taken after powder fracture to illustrate the microstructure (Fig. 2). It is assumed that internalised gas will be stored in the closed internal pores of the coffee, it is important therefore, to understand the relative abundance of the internal and external pores. Powder density was evaluated by three methods: bulk density (simple volumetric density of the powder and surrounding air) (Table 1); powder density (the density of the powder and internal closed pores by helium pycnometry); and crushed density (the density of the powder after crushing by helium pycnometry, which measures the density of the solid component of the powder), and the void density (volume of closed pores per volume of powder) can be calculated by difference (Eq. (1)).

$$\frac{1}{\rho_{VOID}} = \frac{1}{\rho_{POWDER}} - \frac{1}{\rho_{CRUSH}} \quad 1$$

Void density calculation, where ρ_{VOID}, ρ_{POWDER} and ρ_{CRUSH} are used to indicate the void density, powder density and crushed density, respectively.

Bulk density was dependent upon the level of gasification (Table 1) which is further discussed later. For standard coffee, bulk density was 0.278 g/cm^{-3}, powder density was 0.67 g/cm^{-3} and crushed density was 1.6098 g/cm^{-3}. This indicates that the internal volume of the closed pores is 0.88 cm^3/g^{-1}, which can be recalculated on a volume basis and shows that the powder contains 24% v/v closed pores, 17% v/v solid material and the remaining 59% exists as volume between powder particles which is typical of a spray dried instant coffee (Imison, 2011).

It should be noted that scanning electron microscopy images showed no obvious impact of gas internalisation on the microscopic structure at ambient temperature (Fig. 4A) or at elevated temperatures up to 120 °C (Fig. 4B).

3.2. Thermal analysis

Fig. 5 shows a differential scanning calorimeter (DSC) trace for an untreated sample of spray dried coffee which is characteristic of an amorphous material. The step in the heat capacity curve, as indicated by the black arrow, is typical of a glass transition. According to the Ehrenfest thermodynamic classification of phase transitions (Aklonis & MCKnight, 1983) these are thought to be similar to second order transitions, as the step in the heat capacity approximates a discontinuity in a second order derivative of the free energy with respect to temperature. The small overshoot on the top trace is indicative of physical ageing of the sample. This occurs when a sample is stored at a temperature below the nominal glass transition temperature and gradually densifies or ages with time (Gabbott, 2008). A subsequent reheat then reintroduces the energy which is lost on ageing. The glass transition temperature (T_g) is normally measured from the second heating as complications on the trace due to ageing are largely removed and the construction required to obtain a reliable value is much more easily carried out (Fig. 5). The value of T_g recorded in the present experiments is 45 ± 1.0 °C and the value of ΔCp, the step in heat capacity, is 0.34 J/g/°C. (The temperatures that the sample is exposed to during the reheat cycle (>160 °C) exceed, by a substantial margin, that of natural gasification.) According to compositional data approximately 35% of the material is carbohydrate composed of a significant fraction of mono and disaccharides (10%), with the remaining 25% being long chain arabinogalactan

Table 1
Effect of temperature on bulk density of pressurised coffee, different letters indicate significant differences. Significant differences were identified using analysis of variance with Tukey's post hoc test (P<0.05).

Temperature (°C)	Bulk density (g/cm^3)
25	$0.278^{d} \pm 0.005$
60	$0.274^{d} \pm 0.006$
90	$0.327^{cd} \pm 0.004$
100	$0.388^{bc} \pm 0.014$
110	$0.448^{ab} \pm 0.016$
120	$0.488^{a} \pm 0.016$

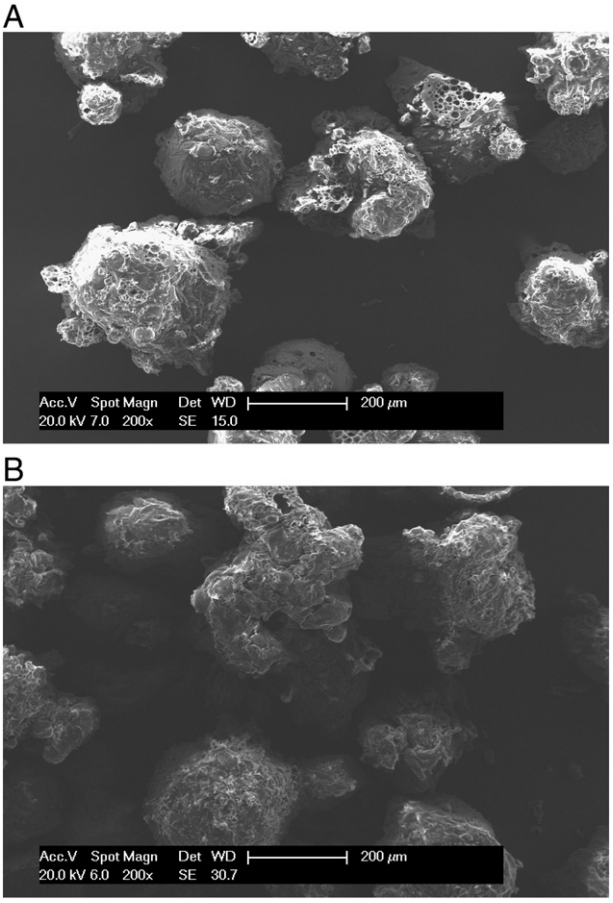

Fig. 4. Scanning electron microscope images of spray dried instant coffee pressurised within a stainless steel pressure cell to 40 bar and then heated to either A) 25 °C or B) 90 °C and allowed to cool to ambient temperature. White scale bar indicates 200 μm.

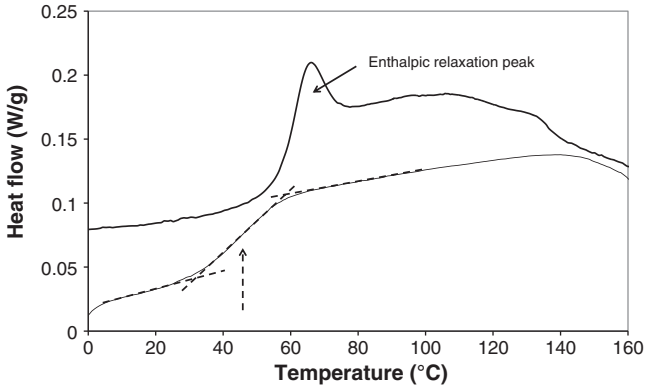

Fig. 5. Differential scanning calorimetry traces for the first heat (top) and reheat. The enthalpic relaxation peak is indicated (solid arrow). The construction (dotted line) used to obtain the glass transition temperature is shown on the reheat with the final value marked (dotted arrow).

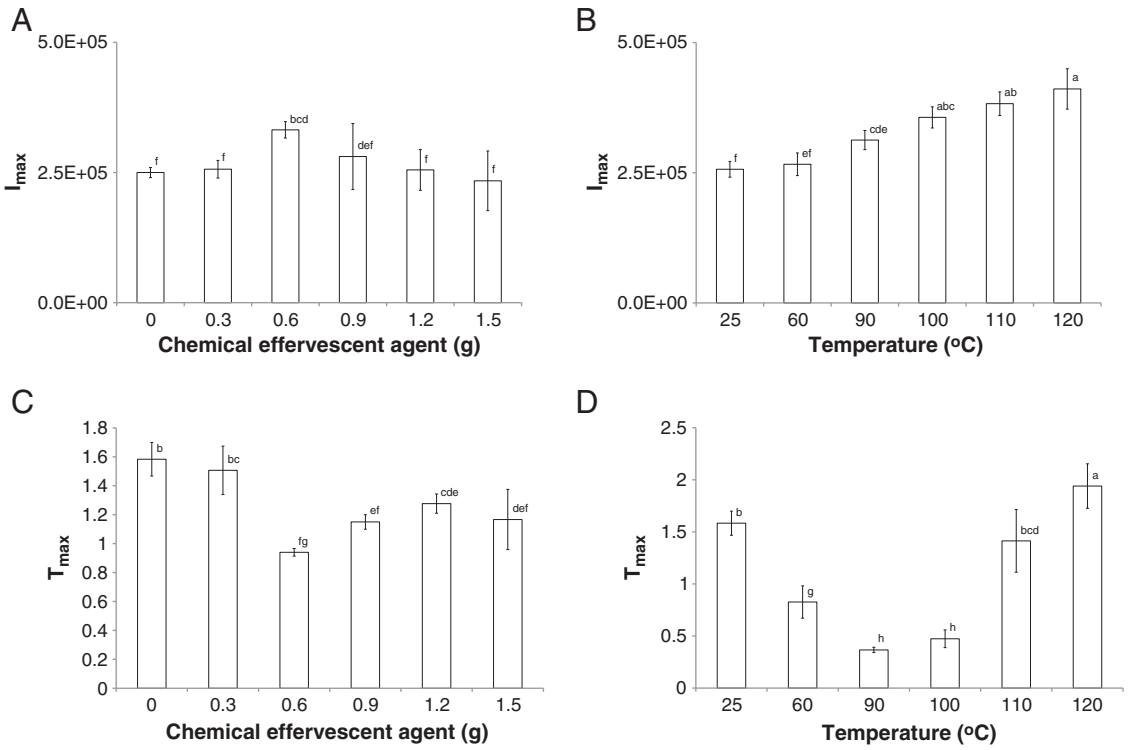

Fig. 6. Effect of the inclusion of chemical effervescent agent (panels A and C) and gas internalisation (panels B and D) on aroma release parameters (I_{max} (panels A and B) and T_{max} (panels C and D)). Different letters indicate significant differences within the data set of one analysis (I_{max} (panels A and B) and T_{max} (panels C and D)). Data points with 0 g chemical effervescent agent represent standard non-treated coffee. All samples contain 1.5 g of instant coffee.

and galactomannan. These DSC values for T_g and ΔCp would suggest a plasticised polymer with significant amounts of other lower molecular weight materials. Measurements have previously been made on the glassy properties of galactomannans (Cerqueira, et al., 2011; Hernández, Ramos, Falcony, & Salazar, 2001) whose T_g values are reported to be dependent on the galactose/mannose ratio and similar to, albeit slightly higher than, the values reported here. ΔCp values appear to be difficult to measure and are much less certain (Chaires-Martínez, Salazar-Montoya, & Ramos-Ramírez, 2008; Hernández et al., 2001).

When considering this type of measurement in the field of volatile and flavour entrapment, there are several properties of the glass transition which must be considered. The first of these is the increased mobility of the matrix above the glass transition temperature (Roos,

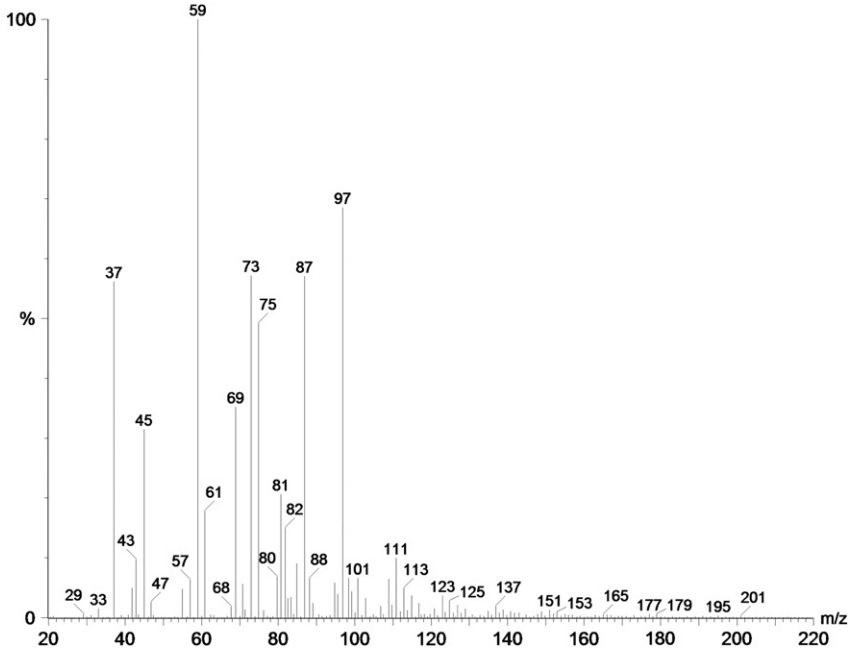

Fig. 7. m/z intensity spectra for a typical coffee sample.

1995). In the schematic illustration in Fig. 1, the penetration of gas into pores occurs when the matrix has enough mobility/high enough diffusivity to allow gas to flow through the walls. This occurs at temperatures substantially above the glass transition temperature. The air introduced at high pressure is believed to be retained within internal voids of the matrix when the sample is subsequently cooled to room temperature and the matrix "sets" at temperatures below the glass transition temperature. It is tempting to imagine that the increased density of air (at pressures of the order of 60 atm) will cause the measured bulk density of the product to increase. However pycnometry results (see previous section and the calculations therein) show that this is unlikely and that changes in the overall bulk density of the samples will be of the order of 0.01–0.02 g/cm^3; which is close to the limit of detectability. What is more likely to be happening is that the increased mobility of the system above T_g is allowing a form of flow under gravity and the progressive densification of the material. This is similar to the collapse experienced by materials during freeze drying (Roos, 1995) when the temperature of the product on the freeze drier shelves exceeds T_g' (the glass transition temperature of the maximally freeze concentrated glass) and the material starts to flow under the influence of gravity, thereby reducing the pore volume and increasing the density. The measured density values for the products considered here increase from 0.278 to 0.488 g/cm^3 (Table 1).

The second important parameter of the glass transition is the explicit time or frequency dependence of the glass transition (Schawe & Höhne, 1996). As the time scale increases or equivalently the frequency of the measurement technique decreases, a lower value of the glass transition temperature will be recorded. Hence the value of the DSC determined T_g which is a comparatively rapid measurement, is not appropriate for storage trials. Therefore temperatures of storage for these materials may have to be substantially lower than the value of 45 ± 1.0 °C reported here in order for them to be stable. Similarly the physical ageing which clearly occurs in these materials, as evidenced by the overshoot on the top trace of Fig. 5, is often associated with embrittlement, increased permeability, poorer entrapment of volatile compounds and higher reaction rates (Hill et al., 2005). This may also be the case here and may impair the shelf life of the stored product. It may therefore be possible to manipulate the composition of the matrix to minimise these effects, for instance by choosing materials (coffee fractions from the soluble coffee process) that are less prone to ageing and densification.

3.3. Delivery of volatile aroma compounds to the headspace during powder hydration

All powders were added at equal coffee loadings in water with no direct contact with the headspace. A mid-range temperature was chosen to slow the dissolution kinetics to a rate that is measurable using current analytical technologies, and to control the atmospheric moisture content. Instant coffee delivered a smooth aroma delivery on hydration, reaching an equilibrium plateau and holding this headspace intensity (Fig. 3). Instant coffee containing the chemical effervescent agent reached an equivalent equilibrium plateau, but did not reach this value in a smooth curve; the peak exceeded the equilibrium value briefly and then returned to the equilibrium value (Fig. 3). Instant coffee containing internalised gas delivered a similar smooth curve to that of the coffee containing chemical effervescent agent (Fig. 3).

The temporal dimension to flavour delivery is important to subsequent overall perception (Xian & Fisk, 2012). Therefore to evaluate the curve shape and profile, two parameters were extracted, I_{max} and T_{max}, which were chosen to be comparable to consumer perception (Shojaei, Linforth, Hort, Hollowood, & Taylor, 2006). I_{max} is defined as the maximum headspace intensity and T_{max} is defined as the time to reach maximum intensity. This was recorded for all samples and is summarised in Fig. 6 for the chemical effervescent agent (I_{max} (Fig. 6A) and T_{max} (Fig. 6B)) and the naturally gasified coffee (I_{max} (Fig. 6C) and T_{max} (Fig. 6D)). I_{max} and T_{max} by APcI-MS are commonly used extraction parameters to understand aroma delivery kinetics (Fisk, 2007; Fisk, Linforth, Taylor, & Gray, 2011a; Taylor & Linforth, 1994).

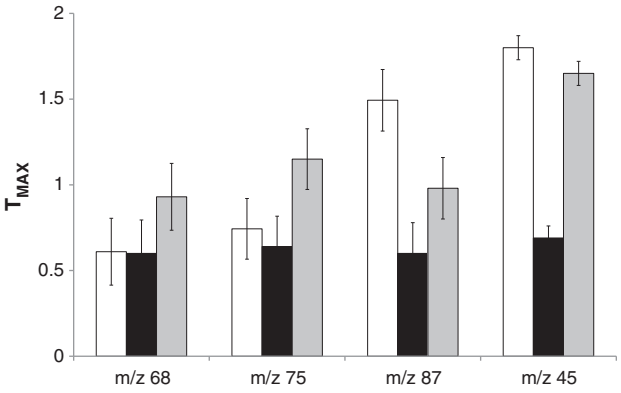

Fig. 8. T_{max} of four ions, pyrrole (m/z 68), pyridine (m/z 80), 2,3 butanedione (m/z 87) and acetaldehyde (m/z 45) for instant coffee (empty bar), pressurised coffee at 90 °C (black bar), and coffee containing chemical effervescent agent.

I_{max} was not impacted by small loadings of effervescent agent, or the application of low temperature pressurised treatment, but was significantly elevated with the application of 0.6 g of effervescent agent or the inclusion of internalised gas at temperatures above 60 °C. Coffee containing internalised gas treated at >110 °C gave a greater I_{max} than the effervescent agent achieved at any loading level, with a 60% increase in headspace intensity achieved with the highest processing temperature of gas internalisation.

The temporal dimension to aroma delivery is critical for the impact of aroma during brewing, Fig. 6 illustrates the change in time to maximum intensity (T_{max}) for both natural gasification and the inclusion of effervescent agent. The use of 0.6 g of effervescent agent reduced the time to maximum intensity from 1.5 min to 0.9 min. If the effervescent agent is replaced with the naturally internalised gas, the time to maximum intensity could be reduced further, from 1.5 min to 0.4 min and 0.5 min for the 90 °C and 100 °C samples respectively. The reduction in T_{max} for samples pre-treated at 90 °C and 100 °C was greater than could be achieved through the use of chemical effervescent agent alone ($P<0.05$), with a 77% reduction in time to maximum headspace aroma intensity.

As the volatile compounds delivered to the headspace have a range of physicochemical properties, one would expect differences in their release rate kinetics; previously Lindinger et al. (2005, 2008) have suggested that specific mass to charge (m/z) ratios can be used to indicate changes in delivery of specific compounds. In this study m/z ratios of 45, 87, 80 and 68 are used to track acetaldehyde, 2,3 butanedione, pyridine and pyrrole, respectively (Fig. 7). The rate of release of each compound varied in the standard instant coffee (Fig. 8) with the T_{max} ranging from 0.6 for pyrrole and 1.8 for

Table 2
Effect of temperature on foam volume stability of pressurised coffee. Foam stability is calculated as percentage of foam present at 1 min still remaining at 10 min.

Temperature (°C)	Foam volume (cm^3)	Foam stability % retained after 10 min
25	5	80%
60	4	75%
90	7	71%
100	9	78%
110	12	75%
120	13	77%

acetaldehyde. There was significant impact of preparation method on the T_{max} for each compound with an acceleration of delivery rate of 2,3 butanedione and acetaldehyde through the use of natural gasification. Of the range of compounds discussed, 2,3 butanedione and acetaldehyde are the most hydrophobic (estimated Log P) which may indicate that the process of natural gasification will selectively accelerate the delivery of individual aroma compounds to the headspace based on their physicochemical properties. This differential delivery rate may be due to the dissolution kinetics being normally limited by solubility issues or hydrophobicity, but when natural gasification is applied the limiting rate kinetic is bypassed due to mixing and the hydrophobic compounds are therefore released more rapidly. The chemical gasification route only accelerated the delivery of 2,3 butanedione, and in one case slowed the delivery rate (pyridine).

When gas bubbles are formed by nucleation or directly injected into a liquid, the large surface area produced allows a rapid saturation of the internal bubble gas by volatile compounds from the continuous liquid phase; this is normally at a static equilibrium level with the media. Although, when locally produced in regions of the media where a dissolving powder is dissolved but not fully dispersed, the local concentrations are significantly elevated and equilibrium occurs relative to this higher concentration, producing bubbles that contain higher than equilibrium concentrations of volatile gases. These super-concentrated bubbles subsequently rise and are released to the headspace leading to a burst of aroma (as shown in Fig. 3). Once dissolution and gas release have been completed the equilibrium state will return.

The formation of bubbles, in addition to modifying the delivery of volatile compounds to the headspace, will also induce the formation of crema (a foam layer on the surface of the coffee brew); when standard instant coffee was hydrated it formed a small crema layer (Table 2) that was stable for 10 min (80% of foam volume was retained). The soluble coffee that had been subjected to natural gasification produced a foam layer that was significantly increased, such that the foam volume was enhanced over standard spray dried coffee by 40% with gasification at 90 °C and doubled by gasification above 100 °C. The foam stability slightly reduced to 71% from 80% (over 10 min) with gasification, but in all samples produced at temperatures of 90 °C or above the crema volume was elevated even after 10 min holding time when compared to standard instant coffee (Table 2).

4. Conclusion

In summary, natural gasification through independent cycling of temperature and pressure allows effective gas entrapment and modification of aroma delivery. Natural gasification not only alters the maximum headspace gas concentration (intensity) but also allows a degree of control over the temporal release dimension (time to maximum aroma headspace intensity) of individual aroma compounds. The development and application of novel flavour delivery tools such as the method described herein will allow product developers a new approach to product formulation and allow greater ingredient flexibility when approaching reformulation challenges (Ubbink & Krüger, 2006).

References

Aklonis, J. J., & MCKnight, W. J. (1983). *Introduction to polymer elasticity*. New York: Wiley.

Baek, I., Linforth, R. S. T., Blake, A., & Taylor, A. J. (1999). Sensory perception is related to the rate of change of volatile concentration in-nose during eating of model gels. *Chemical Senses*, *24*(2), 155–160.

Bhumiratana, N., Adhikari, K., & Chambers, E., IV (2011). Evolution of sensory aroma attributes from coffee beans to brewed coffee. *LWT- Food Science and Technology*, *44*(10), 2185–2192.

Birsperink, C., Ufheil, G., Vuataz, G., & Schoonman, A. J. E. (2004). Foaming ingredient and powder containing it. United States of America Patent US20050287268.

Brown, F., & Diller, K. R. (2008). Calculating the optimum temperature for serving hot beverages. *Burns*, *34*(5), 648–654.

Cerqueira, M. A., Souza, B. W. S., Simoes, J., Teixeira, J. A., Domingues, M. R. M., Coimbra, M. A., et al. (2011). Structural and thermal characterization of galactomannans from non-conventional sources. *Carbohydrate Polymers*, *83*(1), 179–185.

Chaires-Martínez, L., Salazar-Montoya, J., & Ramos-Ramírez, E. (2008). Physicochemical and functional characterization of the galactomannan obtained from mesquite seeds. *European Food Research and Technology*, *227*(6), 1669–1676.

Cilindre, C., Conreux, A., & Liger-Belair, G. (2011). Simultaneous monitoring of gaseous CO(2) and ethanol above champagne glasses via micro-gas chromatography (mu GC). *Journal of Agricultural and Food Chemistry*, *59*(13), 7317–7323.

Clark, R., Linforth, R., Bealin-Kelly, F., & Hort, J. (2011). Effects of ethanol, carbonation and hop acids on volatile delivery in a model beer system. *Journal of the Institute of Brewing*, *117*(1), 74–81.

Cussler, E. L. (1997). *Diffusion: Mass transfer in fluid systems*. Cambridge: Cambridge University Press.

Denker, M., Parat-Wilhelms, M., Drichelt, G., Paucke, J., Luger, A., Borcherding, K., et al. (2006). Investigation of the retronasal flavour release during the consumption of coffee with additions of milk constituents by 'oral breath sampling'. *Food Chemistry*, *98*(2), 201–208.

Dold, S., Lindinger, C., Kolodziejcykt, E., Pollien, P., Ali, S., Germain, J. C., et al. (2011). Influence of foam structure on the release kinetics of volatiles from espresso coffee prior to consumption. *Journal of Agricultural and Food Chemistry*, *59*(20), 11196–11203.

Fisk, I. D. (2007). *Physico-chemical charactorisation of sunflower oil bodies ex-vivo, phd thesis*. University of Nottingham.

Fisk, I. D., Boyer, M., & Linforth, R. (2012). Impact of protein, lipid and carbohydrate on the headspace delivery of volatile compounds from hydrating powders. *European Food Research and Technology*, *235*(3), 517–525.

Fisk, I. D., Kettle, A., Hofmeister, S., Virdie, A., & Silanes Kenny, J. (2012). Discrimination of roast and ground coffee aroma. *Flavour*, *1*(14).

Fisk, I. D., Linforth, R., Taylor, A., & Gray, D. (2011a). Aroma and oil bodies: Potentially a novel delivery route. *XIII Weurman flavour research symposium* Zaragoza.

Fisk, I. D., Linforth, R., Taylor, A., & Gray, D. (2011b). Aroma encapsulation and aroma delivery by oil body suspensions derived from sunflower seeds (*Helianthus annus*). *European Food Research and Technology*, *232*, 905–910.

Fisk, I. D., White, D. A., Lad, M., & Gray, D. A. (2008). Oxidative stability of sunflower oil bodies. *European Journal of Lipid Science and Technology*, *110*(10), 962–968.

Franca, A. S., Mendonça, J. C. F., & Oliveira, S. D. (2005). Composition of green and roasted coffees of different cup qualities. *LWT - Food Science and Technology*, *38*(7), 709–715.

Franks, F. (1988). *Water science reviews 3: Water dynamics*. Cambridge: Cambridge University Press.

Gabbott, P. (2008). *Principles and applications of thermal analysis*. Oxford: Blackwell Publishing Ltd.

Geel, L., Kinnear, M., & de Kock, H. L. (2005). Relating consumer preferences to sensory attributes of instant coffee. *Food Quality and Preference*, *16*(3), 237–244.

Harrison, M., Hills, B. P., Bakker, J., & Clothier, T. (1997). Mathematical models of flavor release from liquid emulsions. *Journal of Food Science*, *62*(4), 653–664.

Hernández, A., Ramos, E., Falcony, C., & Salazar, J. (2001). An approximation to calorimetric analysis on dispersions at different concentrations of mesquite (*Prosopis* sp.) and locus bean (*Ceratonia* sp.) seed gums. *Proceedings of the eighth international congress on engineering and food* (pp. 211–215). USA: Technomic Publishing Company.

Hill, S. A., MacNaughtan, W., Farhat, I. A., Noel, T. R., Parker, R., Ring, S. G., et al. (2005). The effect of thermal history on the Maillard reaction in a glassy matrix. *Journal of Agricultural and Food Chemistry*, *53*(26), 10213–10218.

Imison, T. (2011). *Foaming coffee composition*. United States of America Patent US20110097458.

Jolly, M. D., Nacci, A. T., DeCeglie, G. J., & Vitti, R. A. (1972). *Method for aromatising soluble coffee*. United States of America Patent US4044167.

Jublot, L., Linforth, R. S. T., & Taylor, A. J. (2005). Direct atmospheric pressure chemical ionisation ion trap mass spectrometry for aroma analysis: Speed, sensitivity and resolution of isobaric compounds. *International Journal of Mass Spectrometry*, *243*(3), 269–277.

Kilburn, D., Claude, J., Mezzenga, R., Dlubek, G., Alam, A., & Ubbink, J. (2004). Water in glassy carbohydrates: Opening it up at the nanolevel. *The Journal of Physical Chemistry. B*, *108*(33), 12436–12441.

Kuypers, T. W. (1986). *Process for the manufacture of a frothy drink composition*. United States of America Patent US4748040.

Lefenfeld, M., Berman, S., Berman, J., & Katz, M. (2003). *System for delivery of active substances*. United States of America US20040077513.

Liger-Belair, G., Polidori, G., & Jeandet, P. (2008). Recent advances in the science of champagne bubbles. *Chemical Society Reviews*, *37*(11), 2490–2511.

Lindinger, C., Labbe, D., Pollien, P., Rytz, A., Juillerat, M. A., Yeretzian, C., et al. (2008). When machine tastes coffee: Instrumental approach to predict the sensory profile of espresso coffee. *Analytical Chemistry*, *80*(5), 1574–1581.

Lindinger, C., Pollien, P., Ali, S., Yeretzian, C., Blank, I., & Mark, T. (2005). Unambiguous identification of volatile organic compounds by proton-transfer reaction mass spectrometry coupled with GC/MS. *Analytical Chemistry*, *77*(13), 4117–4124.

Linforth, R. S. T., Pearson, K. S. K., & Taylor, A. J. (2007). In vivo flavor release from gelatin–sucrose gels containing droplets of flavor compounds. *Journal of Agricultural and Food Chemistry*, *55*(19), 7859–7863.

Marin, M., Baek, I., & Taylor, A. J. (1999). Volatile release from aqueous solutions under dynamic headspace dilution conditions. *Journal of Agricultural and Food Chemistry*, *47*(11), 4750–4755.

Maughan, R. J., & Griffin, J. (2003). Caffeine ingestion and fluid balance: A review. *Journal of Human Nutrition and Dietetics*, *16*(6), 411–420.
Narain, C., Paterson, A., & Reid, E. (2004). Free choice and conventional profiling of commercial black filter coffees to explore consumer perceptions of character. *Food Quality and Preference*, *15*(1), 31–41.
Panesar, S. S., Jeffs, W. A., & Turek, E. J. (1999). *Soluble expresso coffee.* Patent US5882717.
Pollien, P., Jordan, A., Lindinger, W., & Yeretzian, C. (2003). Liquid-air partitioning of volatile compounds in coffee: Dynamic measurements using proton-transfer-reaction mass spectrometry. *International Journal of Mass Spectrometry*, *228*(1), 69–80.
Quinlan, P. T., Lane, J., Moore, K. L., Aspen, J., Rycroft, J. A., & O'Brien, D. C. (2000). The acute physiological and mood effects of tea and coffee: The role of caffeine level. *Pharmacology Biochemistry and Behavior*, *66*(1), 19–28.
Roos, Y. (1995). *Phase transition in foods.* London: Academic Press.
Saragoni, P., Aguilera, J. M., & Bouchon, P. (2007). Changes in particles of coffee powder and extensions to caking. *Food Chemistry*, *104*(1), 122–126.
Schawe, J. E. K., & Höhne, G. W. H. (1996). The analysis of temperature modulated DSC measurements by means of the linear response theory. *Thermochimica Acta*, *287*(2), 213–223.
Schoonman, A., Ubbink, J., Bisperink, C., Le Meste, M., & Karel, M. (2002). Solubility and diffusion of nitrogen in maltodextrin/protein tablets. *Biotechnology Progress*, *18*(1), 139–154.
Shojaei, Z. A., Linforth, R. S. T., Hort, J., Hollowood, T., & Taylor, A. J. (2006). Measurement and manipulation of aroma delivery allows control of perceived fruit flavour in low- and regular-fat milks. *International Journal of Food Science and Technology*, *41*(10), 1192–1196.
Taylor, A. J. (1998). Physical chemistry of flavour. *International Journal of Food Science and Technology*, *33*(1), 53–62.
Taylor, A. J., & Linforth, R. S. T. (1994). Methodology for measuring volatile profiles in the mouth and nose during eating. In H. Maarse, & D. G. VanDerHeij (Eds.), *Trends in flavour research*, *Vol. 35*. (pp. 3–14)Amsterdam: Elsevier Science Publ B V.
Taylor, A. J., Linforth, R. S. T., Harvey, B. A., & Blake, B. (2000). Atmospheric pressure chemical ionisation mass spectrometry for in vivo analysis of volatile flavour release. *Food Chemistry*, *71*(3), 327–338.
Ubbink, J., & Krüger, J. (2006). Physical approaches for the delivery of active ingredients in foods. *Trends in Food Science & Technology*, *17*(5), 244–254.
Xian, T., & Fisk, I. D. (2012). Salt delivery from potato crisps. *Food & Function*, *3*(4), 376–380.
Yampolskii, Y. P., Pinnau, I., & Freeman, B. D. (2006). *Materials science of membranes for gas and vapor separation.* England: Wiley.
Zeller, B. L., Ceriali, S., & Gundle, A. (2006). *Foaming soluble coffee powder containing pressurized gas.* : United States of America Patent US 2006/0040038 A1.